



## **SURFACE MOTION EVALUATION OF TERRACE-SHAPED HILL SUBJECTED TO INCIDENT PLANE SV WAVE USING SPECTRAL ELEMENT METHOD**

X. Kong<sup>(1)</sup>, H. Li<sup>(2)</sup>

<sup>(1)</sup> PhD candidate, College of Civil Engineering, Nanjing Tech University, N.200 Zhongshan Road, 210009 Nanjing, China, kongxijun1990@126.com

<sup>(2)</sup> Professor, College of Civil Engineering, Nanjing Tech University, N.200 Zhongshan Road, 210009 Nanjing, China, harbiner@163.com

### ***Abstract***

It has been recognized that effects of the local topographical and geotechnical characteristics are significant on seismic ground motion in the past researches. The terrace-shaped hill is a kind of local irregular topography which is widespread throughout southwest China. In this paper, the spectral element method is employed to investigate the site effects of two-dimensional terrace-shaped hill topography subjected to incident plane P-SV waves. Firstly, the spectral-element model is established on fully quadrilateral meshes to simulate wave propagation by the terrace-shaped hill in a half-space. The wave field is typically represented in terms of high-degree Lagrange interpolants and integrals are computed based upon Gauss-Lobatto-Legendre quadrature which leads to a simple explicit time scheme. Then the amplification of surface motions and the peak ground motion along each grade are calculated, and the seismic site effects of terrace-shaped topography on ground motion are evaluated. Finally, influences of some parameters related to the irregular topography, such as configuration of the terrace, characteristics of soil layers, angles of the incident wave, etc. are investigated. The numerical results show that there exist prominent topographical and geotechnical effects on seismic ground movement amplifications in the irregular configurations.

*Keywords: terrace-shaped hill; seismic site effects; spectral element method*

## 1. Introduction

Topographic irregularities and soil medium have been long studied as two parameters that have significant effects on earthquake ground motion. The research in the last few decades can be divided into two categories: the analytic method and the numerical method. In the literature, Trifunac [1] solved the scattering problem for incident plane SH-waves in a semi-circular canyon with analytic method firstly. Then a series of cases about canyon-shaped and hill-shaped topography by incident SH, P or SV waves were paid attention to, including Wong & Trifunac [2], Lee *et al* [3,4], Yuan & Liao [5], Qiu & Liu [6], Liang *et al* [7]. Studies above only take 2-D problems into consideration. Lee & Zhu [8] figured out how incident plane P-wave travels in 3-D hemispherical canyon. However, both 2-D and 3-D cases solved by analytic method are limited in certain and simple topography because of boundary conditions and function problem, and so on.

Compared with analytic method, numerical method like finite element method (Bao *et al* [9], Rapolla *et al* [10], Koketsu *et al* [11]) can deal with the challenge of boundary conditions in seismic ground motion more easily. The other numerical method such as finite difference method (Olsen *et al* [12]) and boundary element method (Kham *et al* [13]) are also widely used in the past 30 years. Patera [14] proposed the spectral element method (SEM) in computation of fluid dynamics which has the flexibility of the finite element method and good accuracy of pseudo-spectral techniques (Sidler *et al* [15]). Komatitsch *et al* [16] used SEM in 2-D and 3-D seismic wave propagation and provided their code (SPECFEM2D) online for other researchers to study and develop. In the code that will be applied in this paper, the wave field is represented in terms of high-degree Lagrange interpolants and integrals are computed based upon Gauss-Lobatto-Legendre quadrature. As a result, the mass matrix will be perfectly diagonal and a simple explicit time scheme is led to which can save a lot of computer memory. High efficiency of calculation is its advantage, too.



Fig. 1 – (a) Topography of mountains between Sichuan Basin and Chongqing City (geomagnetic coordinate: 29.4°N, 106.4°E; altitude: 160m~379m). The red circle shows the location of Gele Mountain (altitude: 550m~650m). (b) Enlarged view of Gele Mountain on the west of Chongqing City. The black lines describe the cross section of the mountain in a simplified way.

In this article, we simulate the model of terrace-shaped hill based on mountains surrounding Chongqing City (Fig.1a). These mountains are long and distributed in Sichuan Basin where is famous as earthquake-prone areas. Taking the Gele Mountain on west of Chongqing City as reference object, a hill model with two terraces is established (Fig.1b). Considering the length of the mountains, the problem can be seen as plane strain conversion which makes 2-D model more reasonable. Mesh implementation is presented by use of ABAQUS software. The soil region is homogeneous, isotropic and linear-elastic layer. To get the ground acceleration on and around the

hill, Dirac signal is chosen. Influences of some parameters like configuration of the terrace, characteristics of soil layers and angles of the incident wave are investigated. It seems that more and more research has been put on realistic topography (Komatitsch *et al* [17], Lee *et al* [18]) in recent years. Compared with modeling realistic topography, 2-D models in this paper have fewer requirements for hardware and less time to calculate site effects. Suggestions below may be made more likely for similar topography rather than specific topography which can be adopted by editor of code for seismic design of buildings

## 2. Model

### 2.1 Shape

Altitudes of Chongqing City range from 160m to 379m. The Gele Mountain is about 300m higher in altitude that range from 550m to 650m. In the horizontal direction, the width of the mountain is nearly 3000m (Fig.1b). So we build the numerical model shown in Figure.2.

Here, there are two terraces in same size on both sides of the mountain. The topographic shapes are considered as  $L1/L=0$  (Triangle),  $L1/L=0.2$ (Trapezium),  $L1/L=0.4$ (Trapezium),  $L1/L=0.6$ (Trapezium) and  $L1/L=0.8$ (Trapezium) where  $L1$  and  $L$  represent width of the upper surface of the terrace and width of the base of the terrace. Considering the width of the whole mountain is set to 3000m,  $L$  is equal to 750m. Besides, five different height of the terrace represented by  $H$  are considered, i.e.  $H=75,100,125,150,175$ (units: m). Angle of the incident plane SV wave is indicated by symbol  $\alpha$  which plays an important in seismic activity. The influence of topography and incident wave angel on peak ground motion of the surface will be studied in next section.

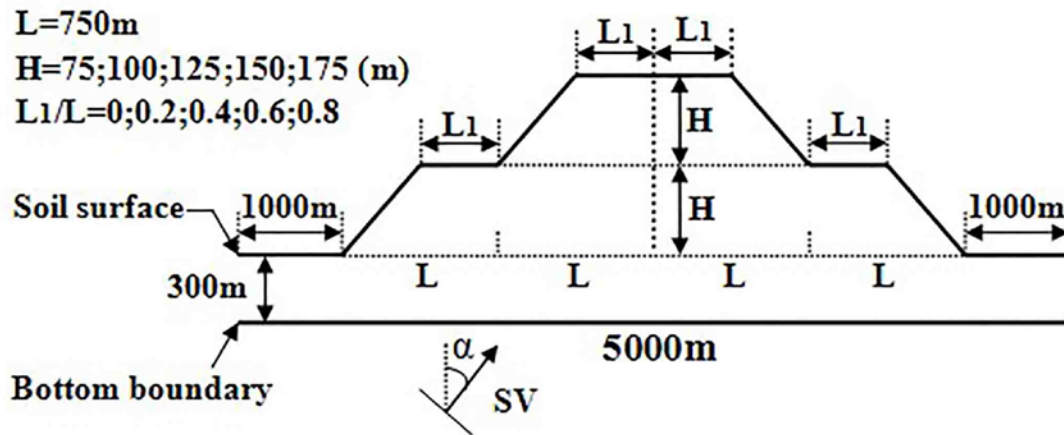


Fig. 2 – Numerical model for 2-D terrace-shaped hill with different topography

### 2.2 Model medium

Table 1 – Parameters of model medium

Category	$P/(\text{kg}/\text{m}^3)$	$E/\text{GPa}$	$\nu$	$Cs/(\text{m}/\text{s})$	$Cp/(\text{m}/\text{s})$
A	2000	0.45	0.25	300	519.6
B	2000	1.25	0.25	500	866
C	2000	2.45	0.25	700	1212.4

( $P$ -mass density;  $E$ -modulus of elasticity;  $\nu$ -Poisson's ratio;  $Cs$ -SV wave velocity;  $Cp$ -P wave velocity)



Gele Mountain is a typical area of karst landform. Soil here is mostly limestone with shear wave velocity about 480 meters per second. To consider the influence of soil characteristic, three different kinds of model medium are constructed in Table 1.

The soil properties of category B in Table 1 are similar to properties of limestone on purpose, to make our simulation closer to reality. If there are no special instructions, soil type B will be used in the computation of seismic wave motion below as the default.

### 2.3 Incident SV wave

For the incident plane SV wave acting on the bottom edge, Dirac function is chosen as the displacement data of ground motion. The source-time function is shown in Figure.3. Its equation in time is given as Eq. (1).

$$f(t) = \begin{cases} 0 ; t < 0 \text{ or } t \geq 0.25 \\ 1024t^3 ; 0 \leq t < 0.0625 \\ 1 - 192t(4t - 0.5)^2 ; 0.0625 \leq t < 0.125 \\ 1 + (192t - 48)(4t - 0.5)^2 ; 0.125 \leq t < 0.1875 \\ -16(4t - 1)^3 ; 0.1875 \leq t < 0.25 \end{cases} \quad (1)$$

where  $t$  is the time;  $f(t)$  corresponds to the displacement data. Duration of the Dirac function is set to 0.25s which can make its frequency range close to seismic waves.

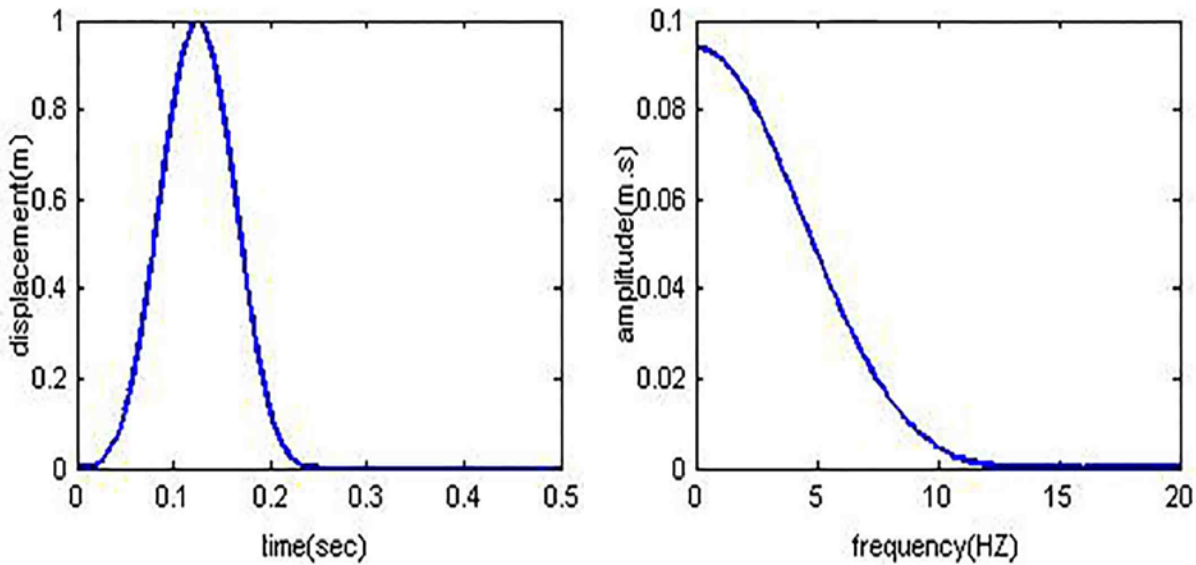


Fig. 3 – The time history and Fourier amplitude spectrum of Dirac impulse

With the impulse wave above loaded on the bottom edge of 2-D terrace-shaped hill model at time zero, total duration of the simulation is set as 6.0 sec. The time step is 0.1 milliseconds, that is, a total of 60000 steps to calculate. The boundary condition applied in the analysis is Stacey boundary condition which will absorb the reflected wave. It is also an important role in calculation of local site ground motion but not the point in this paper.

### 3. SEM Mesh Implementation

In the numerical treatment, the spectral element is used to evaluate the whole system response. According to the research on grid dispersion and stability criteria of SEM for elastic wave equations by Basabe & Sen [19], dispersion is less than 0.2% at four to five nodes per wave length. Multiplying duration of the Dirac function ( $T=0.25s$ ) and shear wave velocity ( $C_s \geq 300m/s$ ), wave length in our simulation will be at least 75 meters. Degree of the Gauss-Lobatto-Legendre (GLL) basis functions used in this paper is 4 which mean there are 5 GLL points on each edge of a quadrangle element and 25 points in each spectral element. As a result, size of the element can not be larger than 75 meters. The SPECSEM2D package provided by Komatitsch and run in this paper can't offer mesh service. But there is a lot of mesher in the market such as GID, ABAQUS or CUBIT that can provide the mesh data need in the code. Here, we make use of ABAQUS software to generate mesh which is shown in Figure.4 as an example. To ensure a good accuracy of the result, size of mesh is 10 to 20 meters.

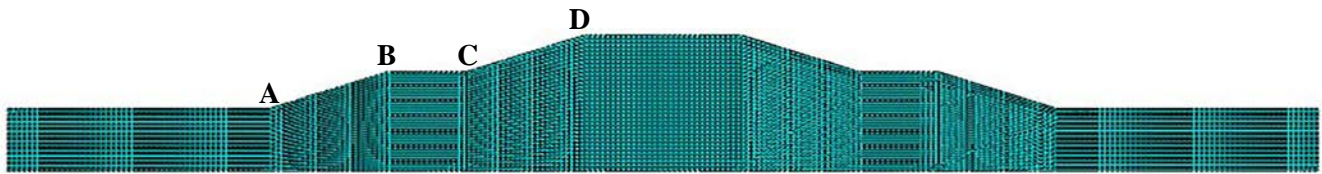


Fig. 4 – Mesh of the 2-D terrace-shaped hill

As we build the model with different topography, the numbers of spectral elements range from 4469 to 8448. The amount of computer memory in simulation of this paper is 32G that is enough. As mentioned above, the time step is 0.1 msec. It takes about 40 min for the calculation with duration of 6 sec under different conditions. The horizontal distance between the receivers we set on the surface is 25 m.

### 4. Parametric Studies and Discussion

To analyze the seismic site effects of the 2-D terrace-shaped hill, peak ground displacement of the surface is observed. In section 2, we build the model in 3 steps. Correspondingly, the influence of topography, characteristics of soil layers and angles of the incident wave will be studied in this section.

#### 4.1 Topography

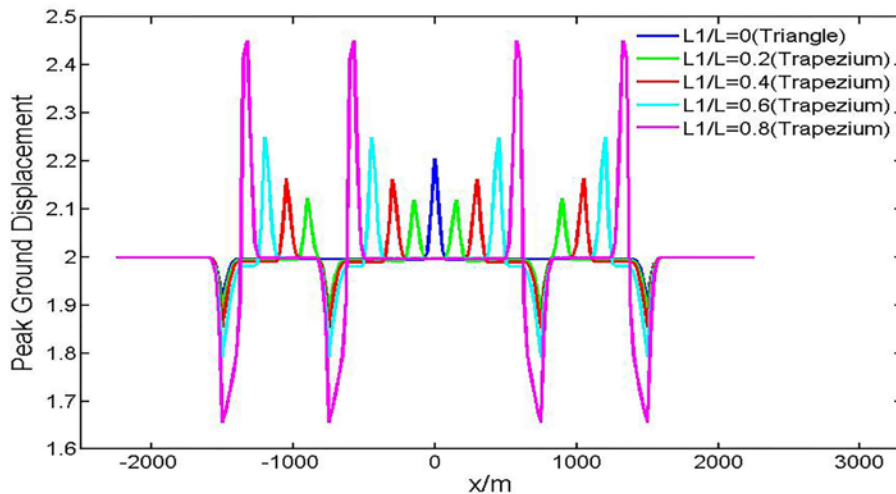


Fig. 5 – Influence of surface shape on horizontal displacement for  $L1/L=0$ ,  $L1/L=0.2$ ,  $L1/L=0.4$ ,  $L1/L=0.6$  and  $L1/L=0.8$  ( $H=75m$ )



Figure.5 shows the influence of surface shape on horizontal displacement for  $L1/L=0$  (triangle) and  $L1/L=0.2\sim 0.8$  (trapezium) while the height of the terrace is 75 m (the width  $L1$  varies while  $L$  remains constant). According to the results, peak ground displacements are strongly affected by the topography. For the triangle case of the terrace ( $L1/L=0$ ), peak ground displacements in horizontal direction at the top of the hill increase by about 10 percent and decrease by about 5 percent at the foot. For the trapezium case of the terrace, PGD increase when the site is at the upper point of the slope (point B and point D), but decrease at the lower point of the slope (point A and point C). The amplitudes of displacement depend on the site of the surface and  $L1/L$  ratio. It is shown that PGD of the surface remain unchanged as 2.0 outside the range of 50 m with the points marked in figure 4 (point A, B, C, D). Within the range, PGDs of point B and point D are same as the largest while PGDs of point A and point C are same as the lowest. The changing trends decrease when the distance with these points increase. While  $L1/L$  ratio gets increases from 0.2 to 0.8, the increased percentages (point B and point D) change from 5.9 per to 22.5 per and the decreased percentage (point A and point C) change from 5.6 per to 17.1 per.

Figure.6 shows the influence of the surface shape on horizontal displacement for five different heights ( $H=75m$ ,  $H=100m$ ,  $H=125m$ ,  $H=150m$  and  $H=175m$ ) while the width of the upper surface of the terrace  $L1$  remains as 300m. The results show that the variation tendency for PGD of those corner points grows when the height of the terrace increase. Table 2 provides the value of maximum PGD on surface under different conditions. It is shown that the maximum PGD on surface increases while the height  $H$  increases.

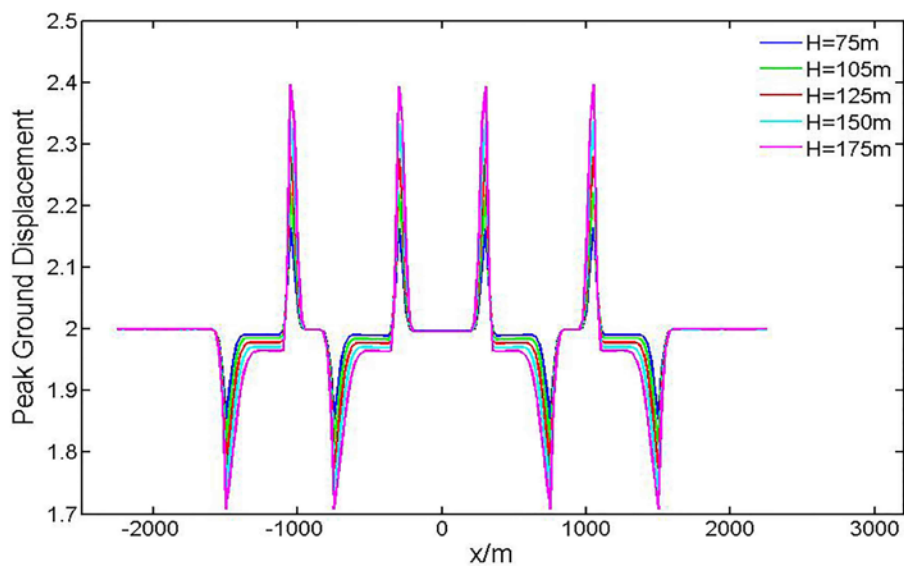


Fig. 6 – Influence of surface shape on horizontal displacement for  $H=75m$ ,  $H=100m$ ,  $H=125m$ ,  $H=150m$  and  $H=175m$  ( $L1/L=0.4$ ;  $L1=300m$ )

Table 2 – Maximum peak ground displacement on surface with different height of the terrace

<b>H</b>	<b>75m</b>	<b>100m</b>	<b>125m</b>	<b>150m</b>	<b>175m</b>
PGD(max)	2.165	2.222	2.279	2.337	2.396

#### 4.2 Soil characteristics

Figure.7 shows the influence of soil characteristics on horizontal displacement. Three different kinds of soil are investigated. To explain briefly, mass density and Poisson’s ratio of the soil are set as constant while modulus of elasticity varies. Only one shape of terrace model ( $H=100m$ ,  $L=300m$ ) is taken into account in this subsection. It seems that PGD on surface has a small increase when the modulus of elasticity increases. In Table 3, maximum



of the PGD (point B or point D) on surface is provided. The difference ratio of PGD between the three soils is less than 0.5 percentages. According to Snell’s law in seismology, the amplification coefficient of displacement or acceleration on regular surface is same when the SV wave whose incidence is vertically propagates from the bottom in one-phase elastic media. So, the results get as Figure.7 and Table 3 are reasonable. The little difference is mainly caused by the reflection of the irregular topography.

But considering the complexity of actual soil, effects of soil characteristics on seismic wave propagation can not be ignored. Due to the limitation of length, this article won’t put more effort on it.

Table 3– Maximum peak ground displacement on surface with different height of the terrace

Category	A (E=0.8Gpa)	B (E=1.25Gpa)	C (E=1.8Gpa)
PGD(max)	2.2161	2.2218	2.2223

(mass density and Poisson’s ratio remain constant :  $P = 2000 \text{ kg/m}^3, \nu = 0.25$  )

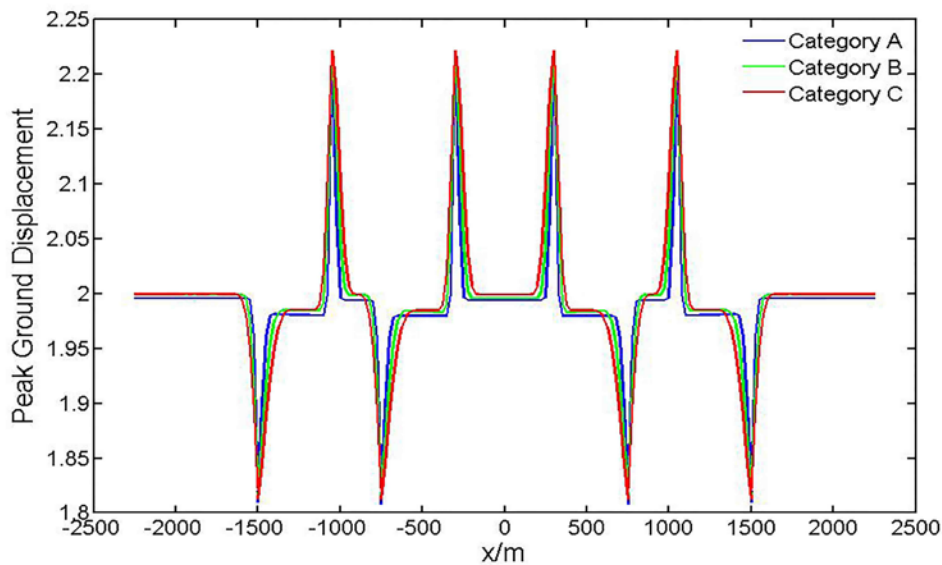


Fig. 7 – Influence of soil characteristics on horizontal displacement for H=100m, L=300m

#### 4.3 Angles of incident wave

Figure.8 shows the influence of incident angles on horizontal displacement. From Table 4, we can get the maximum horizontal displacement under the three conditions. In general, horizontal displacement on surface in oblique waves is smaller than that in waves whose incidence is vertically. We can find the same results at most sites on surface in figure 8. But when the incident angle is 30 degrees, horizontal displacements around point D on the right side are bigger than the results when incident angle are 0 or 15 degrees. Multiple reflection and refraction in the space of terrace-shaped hill can be clearly observed in Figure.9.

Table 4 – Maximum horizontal displacement on surface with different incident angles

Incident angle	0°	15°	30°
PGD(max)	2.2218	2.1894	2.8504

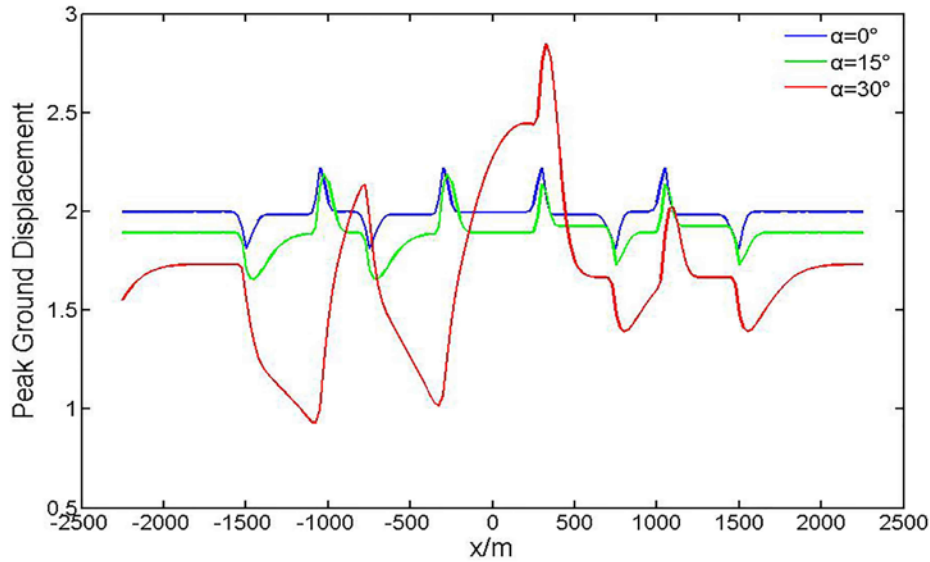


Fig. 8 – Influence of incident angles on horizontal displacement for  $H=100\text{m}$ ,  $L=300\text{m}$

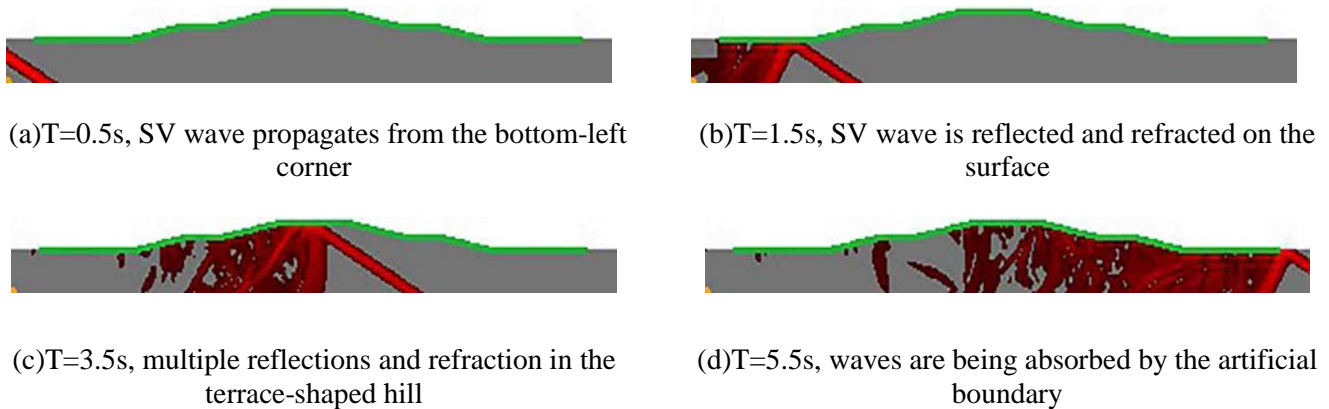


Fig. 9 – Snapshot of wave field when SV wave whose incident angle is 30 degree propagates from the bottom-left corner

## 5. Conclusion

By using spectral element method, we carry out a parameter study for 2-D terrace-shaped hill to characterize site effects in wave propagation with incident SV wave. Effects of topography, soil characteristics and wave's incident angle on peak ground displacement of surface are evaluated. The results show that these parameters play an important role in dynamic behavior of the system. We can conclude that: (a) ground displacement is amplified around the raised corner of the terrace (point B and point D) with the distance in 50 meters, but it is attenuated around the depressed corner of the terrace (point A and point C) within 50 meters; (b) PGD amplifications get stronger when  $L1/L$  ratio or height  $H$  increases as the slope become steeper; (c) considering the model medium is one-phase elastic, only a little increase of PGD happens when soil goes hard. It will be the following research to consider the realistic soil; (d) because of the multiple reflections and refractions on the irregular surface, angle of incident wave has significant influence on ground motion. It should be considered when we do seismic design under irregular topographies.



## 6. References

- [1] Trifunac MD (1972): Scattering of plane SH waves by a semi-cylindrical canyon. *Earthquake Engineering & Structural Dynamics*, **1** (3), 267-281.
- [2] Wong HL, Trifunac MD (1974): Surface motion of a semi-elliptical alluvial valley for incident plane SH waves. *Bulletin of the Seismological Society of America*, **64** (5), 1389-1408.
- [3] Lee VW (1984): Three dimensional diffraction of plane P, SV & SH waves by a hemispherical alluvial valley. *Soil Dynamics & Earthquake Engineering*, **3** (3), 133-144.
- [4] Lee VW, WU X (1994): Application of the weighted residual method to diffraction by 2-D canyons of arbitrary shape: II. incident P, SV & Rayleigh waves. *Bulletin of the Seismological Society of America*, **13** (5), 365-375.
- [5] Yuan X, Liao ZP (1996): Surface motion of a cylindrical hill of circular-arc cross-section for incident plane SH waves. *Soil Dynamics & Earthquake Engineering*, **15** (3), 189-199.
- [6] Li W, Zhao C (2005): Scattering of plane SV waves by cylindrical canyons in saturated porous medium. *Soil Dynamics & Earthquake Engineering*, **25** (12), 981-995.
- [7] Liang J, Zhang Y, Lee VW (2006): Surface motion of a semi-cylindrical hill for incident plane SV wave's analytical solution. *Acta Seismologica Sinica*, **19** (3), 251-263.
- [8] Lee VW, Zhu G (2014): A note on three-dimensional scattering and diffraction by a hemispherical canyon-1: vertically incident plane P-wave. *Soil Dynamics & Earthquake Engineering*, **61-62**, 197-211.
- [9] Bao H, Bielak J, Ghattas O (1998): Large scale simulation of elastic wave propagation in heterogeneous media on parallel computers. *Computer Methods in Applied Mechanics & Engineering*, **152** (1-2), 85-102.
- [10] Rapolla A, Bais G, Bruno PPG, Fiore VD (2002): Earth modeling and estimation of the local seismic ground motion due to site geology in complex volcanoclastic areas. *Annals of Geophysics*, **45** (6), 779-790.
- [11] Koketsu K, Fujiwata H, Ikegami Y (2004): Finite element simulation of seismic ground motion with a voxel mesh. *Pure & Applied Geophysics*, **161** (11), 2183-2198.
- [12] Olsen KB, Madariaga R, Archuleta RJ (1997): Three dimensional dynamic simulation of the 1992 Landers earthquake. *Science*, **278** (5339), 834-838.
- [13] Kham M, Semblat JF, Romdhane NB (2013): Amplification of seismic ground motion in the Tunis basin: Numerical BEM simulations vs experimental evidences. *Engineering Geology*, **155**, 80-86.
- [14] Patera AT (1984): A spectral element method for fluid dynamics: Laminar flow in a channel expansion. *Journal of Computational Physics*, **54**, 468-488
- [15] Sidler R, Carcione JM, Holliger K (2013): A pseudo-spectral method for the simulation of poro-elastic seismic wave propagation in 2D polar coordinates using domain decomposition. *Journal of Computational Physics*, **235**, 846-864
- [16] Komatitsch D, Vilotte JP, Vai R, Covarrubias JMC, Sesma FJS (1999): The spectral element method for elastic wave equations-application to 2-D and 3-D seismic problems. *International Journal for Numerical Methods in Engineering*, **45** (9), 1139-1164
- [17] Komatitsch D, Liu Q, Tromp J, Suss P, Stidham C, Shaw JH (2004): Simulations of ground motion in the Los Angeles basin based upon the spectral element method. *Bulletin of the Seismological Society of America*, **94** (1), 187-206.
- [18] Lee SJ, Chen HW, Liu Q, Komatitsch D, Huang BS, Tromp J (2008): Three dimensional simulations of seismic-wave propagation in the Taipei basin with realistic topography based upon spectral-element method. *Bulletin of the Seismological Society of America*, **98** (1), 253-264.
- [19] Basabe JDD, Sen MK (2007): Grid dispersion and stability criteria of some common finite-element methods for acoustic and elastic wave equations. *Geophysics*, **72** (6), T81-T95